AGU100 ADVANCING EARTH AND SPACE SCIENCE

JGR Space Physics

Key Points:
- Sensitivity of noctilucent cloud (NLC) observable properties on condensation nuclei (CN) concentration depends on vertical wind amplitudes
- Ice mass density is directly related to CN concentration when large vertical winds are present
- Under sedimentation and diffusion dominated conditions the observable NLC properties show limited sensitivity

Correspondence to:
H. Wilms,
henrike.wilms@dlr.de

Reply to Comment on "Nucleation of Mesospheric Cloud Particles: Sensitivities and Limits"

H. Wilms[1] (ID) **, M. Rapp[1,2]** (ID) **, and A. Kirsch[3]**

[1]Deutsches Zentrum für Luft- und Raumfahrt, Institut für Physik der Atmosphäre, Oberpfaffenhofen, Germany, [2]Meteorologisches Institut München, Ludwig-Maximilians-Universität München, Munich, Germany, [3]Leibniz Institute of Atmospheric Physics, Kühlungsborn, Germany

Abstract A comment by Megner (2019; M19) aims at resolving the discrepancies between the results of Megner (2011, https://doi.org/10.1016/j.jastp.2010.08.006; M11) and Wilms et al. (2016, https://doi.org/10.1002/2015JA021764; WRK16). M11 concluded that the observable properties of noctilucent clouds are close to insensitive to the concentration of meteoric smoke particles (MSPs), whereas WRK16 concluded that there is a sensitivity. M19 argues that the differences arise due to the different ranges of MSP number densities, which were analyzed in the two studies. Additionally, M19 claims that both studies show a limited sensitivity when the number density of condensation nuclei is 100 cm^{-3} or more. However, this is not confirmed in our simulations. We show that the range of MSP number densities in WRK16 is similar to the range considered by M11. In this range, the simulations of WRK16 are highly sensitive to the number of MSPs: Observable properties such as ice column mass are linearly related to the number of available condensation nuclei. We explain the different sensitivities by different vertical wind amplitudes. Our results suggest that the relative contribution of vertical wind and vertical diffusion to the vertical transport of mesospheric ice particles is the decisive factor. If vertical diffusion dominates, as in M11, there is only limited sensitivity. If vertical wind dominates, as in WRK16, noctilucent cloud properties are directly coupled to the nucleation conditions.

1. Introduction

The nucleation process of noctilucent clouds (NLCs) is not yet understood in detail. Furthermore, there seems to be disagreement on how the number density of meteoric smoke particles (MSPs; N_{MSP}) influences the observable properties of NLCs, even when considering the same theoretical framework of classical nucleation theory. The question how the observable NLC properties depend on N_{MSP} was first studied systematically by M11 where she concluded that "the observable quantities of NLCs, such as ice mass and cloud brightness, are much less sensitive to the concentration of CN [condensation nuclei] than what previously has been believed." In our study (WRK16) we came to the conclusion that there is a "clear relationship between initial MSP number density or nucleation conditions, in general, and the observed NLC properties." In a comment on WRK16, M19 argues that the differences are smaller than they first appear. According to M19, the bulk properties of NLCs exhibit a limited sensitivity on CN number density in both studies, in particular for CN number densities larger than 100 cm^{-3}. Below that threshold of 100 cm^{-3} M19 finds a weak sensitivity. M19 assumes that we came to our conclusion because we tested for a wider range of CN number densities and thus saw more of the regime where there is a weak sensitivity. In the following we analyze whether there is indeed a range of only limited sensitivity in our simulations presented in WRK16.

To facilitate the following discussion, Figure 1 illustrates the mechanism of NLC development as inferred from the studies of M11 and WRK16. In both studies, ice particles nucleate at the mesopause, but the subsequent transport and growth of the ice particles differ. In the simulations of M11 only few of the ice particles from the nucleation region reach the so-called "growth region." The main mechanism for the vertical transport is vertical diffusion. By this mechanism, the ice particle population in the growth region (the observable part of the cloud) is decoupled from the population in the nucleation region. Thus, the observable NLC properties are independent of N_{MSP}. A completely different picture is derived from the simulations of WRK16: After nucleation, the whole population of ice particles is transported to lower altitudes by the large vertical wind induced by gravity waves. During this time, the ice particles grow collectively until they become visible. All ice particles are equally affected by the vertical wind because there is no size dependence as for sedimen-
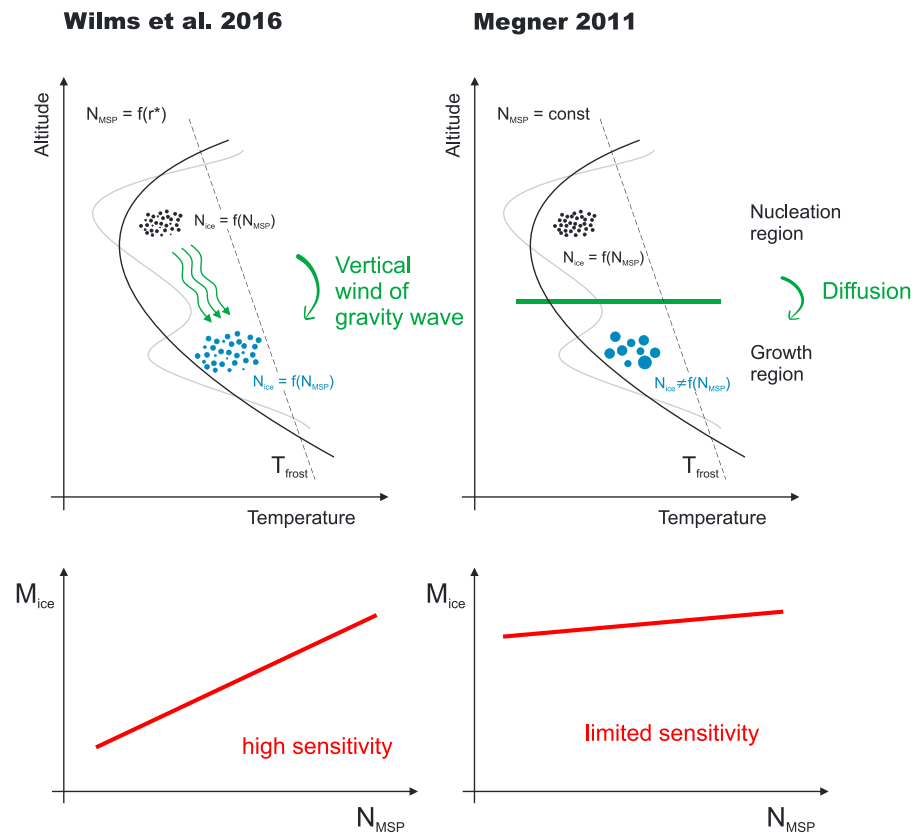
Figure 1. Sketch of noctilucent cloud development in the simulations of WRK16 (left) and M11 (right). The dominant transport mechanism in WRK16 is the vertical wind, whereas diffusion dominates the transport in M11. WRK16 find a linear dependence between N_{MSP} and M_{ice}, whereas there is only limited sensitivity in M11 (lower part). MSP = meteoric smoke particle.

tation. Therefore, the number density of ice particles N_{ice} in the visible part of the cloud is directly related to the number of ice particles nucleated at the mesopause and consequently also to N_{MSP}. The basic assumption of the study of M11 is that "a certain percentage of the super-saturated water vapor is converted to ice" so that "the total ice mass, M_{ice}, is only a function of the local atmospheric conditions and as such independent of the number of CN" (M11). This assumption is depicted in the lower right part of Figure 1 where the ice mass density depends only slightly on N_{MSP}. The simulations of WRK16 suggest a linear dependence between N_{MSP} and M_{ice}.

2. Relationship Between N_{MSP} and N_{ice}

There are fundamental differences between the initial MSP size distribution used in M11 and WRK16: While the simulations of M11 were initialized with MSPs of the same size (1 nm), we used the MSP size distributions of Hunten et al. (1980) and Megner et al. (2008) in WRK16. For a rough comparison with M11, we stated the number density of MSPs larger than 1 nm ($\tilde{N}_{MSP}$). However, $\tilde{N}_{MSP}$ does not indicate the maximum number density of ice particles in the simulations of WRK16. Instead, the number density of ice particles is determined by the number density of MSPs which are larger than the so-called critical radius $r*$ (Pruppacher & Klett, 1997; Rapp & Thomas, 2006). Since the critical radius is temperature dependent and can be smaller than 1 nm, MSPs which are smaller than 1 nm can also be activated. This difference makes it difficult to compare the absolute numbers of CN between M11 and WRK16.

This ambiguity is partly resolved in M19, where an additional simulation for the Hunten size distribution is added to Figure 1. As stated by M19, the NLC properties obtained from her simulation with the Hunten distribution closely follow the simulation with the monodisperse MSP size distribution of $N_{MSP} = 10^4 \, \text{cm}^{-3}$ (yellow line). This provides a link between the two studies, because the Hunten size distribution is the reference case of our Figure 11 in WRK16. Since we scaled the Hunten profile by factors between 10^{-3}
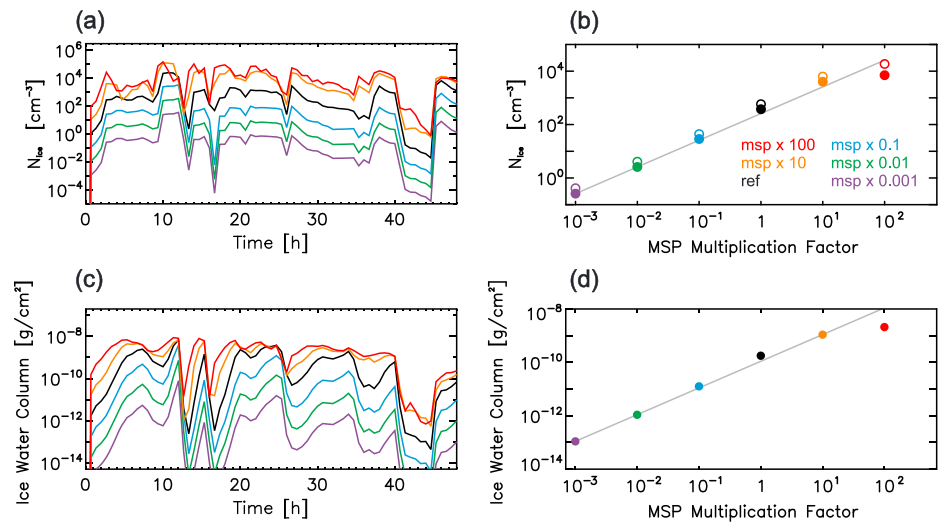
Figure 2. (a) Time series of N_{ice} at the altitude of maximum cloud brightness for different MSP number densities (MSP profile of Megner et al., 2008, multiplied with factors between 0.001 and 100, see panel (b) for reference to the colors). (b) Median of the time series in panel (a) as full circles and median of a time series of maximum N_{ice} as empty circles. (c) Time series of the ice water column. (d) Median value of the time series from panel (c). Straight lines in (b) and (d) denote unity slopes. MSP = meteoric smoke particle.

and 10^2, our range corresponds to roughly $N_{MSP} = 10^1\,cm^{-3}$ to $N_{MSP} = 10^6\,cm^{-3}$ in a monodisperse size distribution. We thus covered the complete range studied in M11 and extended it by one order of magnitude to both smaller and larger CN number densities. The actual CN numbers densities might be even larger in our simulations, since the temperature fluctuations in our background fields are slightly larger than in M11 and the critical radius is thus smaller compared to M11. It is therefore, in our opinion, not correct that we "tested the sensitivity to lower CN densities and lower nucleation rates than I [M19] considered likely" (M19).

In the following we show results of microphysical simulations of mesospheric ice particles which were already presented in WRK16. These simulations were obtained with the Community Aerosol and Radiation Model for Atmospheres (CARMA) in a one-dimensional setup with gravity wave perturbed background fields from the Kühlungsborn Mechanistic general Circulation Model (Becker, 2009; the background fields are provided as supporting information). In contrast to Figure 11 in WRK16, we now show results based on the MSP size distribution of Megner et al. (2008), because this size distribution takes into account the meridional transport of MSPs away from the summer pole (see also Hervig et al., 2009a) and is thus more physical. Figure 2a shows the number density of ice particles N_{ice} as a function of time at the altitude of maximum cloud brightness. The median of the time series of panel (a) is shown in panel (b) as full circles. Empty circles correspond to the equivalent analysis performed with the maximum N_{ice} per profile (instead of N_{ice} at the altitude of maximum brightness as in (a)). The empty circles thus correspond to N_{ice} values representative of the nucleation region.

In our simulations there is a linear relationship between N_{MSP} and N_{ice} for almost the complete range of N_{MSP}. This linear relationship is valid for the nucleation region (empty circles) as well as for the visible part of the cloud (full circles). More importantly, N_{ice} changes only by a factor of 1.5 between nucleation region and the visible part of the cloud. The observable cloud properties are thus directly coupled to the properties of the nucleation region and the number of MSPs, as sketched in the left part of Figure 1. M19 finds a linear relationship between N_{MSP} and N_{ice} for the nucleation region, but not for the visible part of the cloud. Her simulations show that at the largest CN concentration only about 1/100 of the nucleated ice particles reach the lower part of the cloud. This is independent of whether constant or gravity wave perturbed vertical winds were used.

Figure 2c shows the temporal evolution of the ice water column (M_{ice}) as well as the median value of M_{ice} in Figure 2d. All simulations (except "MSP × 100") fall onto the line with unity slope. These simulations can therefore be clearly attributed to a sensitive (or linear) regime, where the observable NLC property M_{ice}
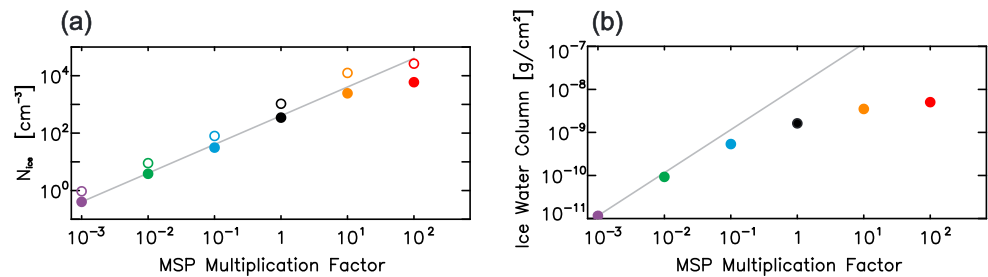
Figure 3. (a) Median ice particle number density and (b) median ice water column as in Figure 2 but from simulations with vertical wind amplitudes reduced by a factor of 2. MSP = meteoric smoke particle.

is directly related to the number density of available CN. This sensitivity is not found in the simulations of M19, where a thousandfold increase in CN leads to only a doubling of the ice mass. Including vertical wind variability in M19 gives a slightly more linear relationship, but with a slope much smaller than unity. In these simulations a 10^4-fold increase in CN concentration leads to only a fourfold increase in M_{ice}.

It is therefore justified to claim that—in the simulations of M11 and M19—there is only limited sensitivity of the observable NLC properties on the number of CN. However, our simulations clearly indicate a very sensitive relationship between the number of available CN and ice mass and ice particle number density in the observable part of the cloud. We do not find a transition at $N_{ice} \approx 100\,cm^{-3}$, as proposed by M19. Instead, we find a linear relationship throughout the whole range of analyzed MSP number densities. Thus, we do not agree on the conclusion of M19, that the results presented in M11 and WRK16 are rather similar and show a limited sensitivity.

2.1. Influence of Vertical Wind Amplitudes

The comparison between Figure 2b of this paper and Figure 2c of M19 clearly demonstrates that the vertical transport of ice particles differs fundamentally between the simulations of M11 and WRK16. Another point to note is that the absolute values of M_{ice} in Figure 2 are significantly smaller than in M19. We already discussed in WRK16 that the vertical wind limits the life time of ice particles in our simulations and that a reduction of the vertical wind amplitude increases NLC brightness and presumably also M_{ice}. Both arguments together suggest that the amplitude of the vertical wind is the deciding difference between the simulations of M19 and WRK16. Indeed, the root-mean-square (RMS) values of the vertical wind are about 0.5 m/s in WRK16 (see Figure 3 of WRK16), whereas they are only 0.15 m/s in M11 and M19.

For testing the hypothesis that the vertical wind amplitudes are the deciding difference, we repeat the simulations shown in Figure 2 with reduced vertical wind amplitudes. For these simulations we scaled the vertical wind perturbations with a factor of 0.5. These simulations were not included in WRK16, but are based on the exact same model setup. Note that in these simulations, the temperature field is not modified, so that wind and temperature perturbations are not consistent according to gravity wave polarization relations. However, in this section, we analyze the effect of smaller vertical winds on the transport of ice particles and want to leave the nucleation condition, that is, the temperature, unchanged. The median N_{ice} and M_{ice} values of these simulations are shown in Figure 3.

The median ice number density shows a linear dependence on the CN number density (panel a). However, the difference between N_{ice} in the nucleation region (empty circles) and the N_{ice} in the observable part of the cloud (full circles) increased compared to the simulations with original vertical wind amplitudes. Furthermore, the ratio of both number densities increases with increasing N_{MSP} and is roughly a factor two to three larger compared to Figure 2b. In simulations with even smaller vertical wind amplitudes (w scaled by 0.1, not shown), N_{ice} differs by up to one order of magnitude between the nucleation region and the observable part of the cloud. The median ice water column (panel b) shows a clear deviation from the linear relationship which was found above. In the simulations with reduced vertical wind, M_{ice} seems to approach an upper bound close to 10^{-8} g/cm³. This upper bound is very similar to the maximum ice column masses obtained in M19. For low CN number densities, that is, MSP multiplication factors 0.1 and less, we find a linear regime. For larger MSP multiplication factors, there is almost no dependence of M_{ice} on the number density of CN. From panel a it can be inferred that the transition occurs between median ice number densities in the nucleation region of 10^2 and $10^3\,cm^{-3}$. In the simulations of M19 this transition occurs at

$N_{ice} \approx 10^2 \, cm^{-3}$. Thus, by reducing the vertical wind amplitude we obtain results which show similar tendencies as the results of M19: (1) linear regime for low CN concentrations and limited sensitivity for high CN concentrations, (2) increasing difference between N_{ice} in the nucleation region and the observable part of the cloud with increasing CN number density.

Combining the results and discussions from M11, WRK16, M19, and this study, the following physical mechanism evolves: Three different processes contribute to the vertical transport of ice particles at the polar summer mesopause, namely, sedimentation, diffusion, and vertical wind. If the vertical wind dominates, the whole ice particle population is transported from the nucleation region to the lower part of the NLC and the observable properties are directly coupled to the nucleation conditions. This is the case in WRK16. In the case of only mean vertical winds and when the sedimentation velocity does not overcome the vertical wind, diffusion is the main driver for bringing part of the ice particles down to the growth region, as described in M11. In such a situation, the observable cloud properties are decoupled from the processes in the nucleation region. The simulations of M19 including gravity wave perturbed wind fields and our simulations with reduced wind amplitudes give results which lie in between the two extreme cases. This suggests that the relative contribution of (a) sedimentation and diffusion and (b) vertical wind to the total vertical transport is deciding. With dominating vertical wind fluctuations, observable NLC properties would strongly depend on the number of available CN, whereas with dominating diffusion, there would be no to little dependency. Additionally, in background fields with no or little vertical wind perturbations, the ice particles have a sufficiently long residence time in the supersaturated region to deplete the available water vapor. Therefore, an upper limit of M_{ice} exists which is independent of N_{MSP}. However, rapidly changing winds prevent a steady state where all available water is converted to ice. This leads to a lower M_{ice} compared to simulations with constant vertical wind. Thus, the "certain percentage of the supersaturated vapor" (M11) which is converted to ice most likely depends on the background conditions and in particular on the amplitude of vertical wind perturbations.

The transport velocities due to diffusion and wind are most likely not independent from each other. Large amplitude gravity waves are prone to breaking, thus leading to turbulence and enhanced eddy diffusivity. Therefore, large vertical winds might be related to strong diffusion. This interrelationship is not included in our simulations and presumably not in the simulations of M11.

3. Nucleation and Growth Region

Since observations of vertical winds in the mesopause region are sparse (see WRK16 for a summary of a few observations), we try to find observational evidence for either the sedimentation-diffusion concept pursued by M11 and M19 or the vertical wind concept inferred from our simulations.

Our following arguments are based on the assumption that the altitude region of the largest backscatter coefficient β_{max} coincides with the altitude region of maximum ice mass density. This assumption is based on their almost equal mean altitudes which are found in observations: The mean centroid NLC height based on the backscatter coefficient determined by lidar measurements at ALOMAR (69°N) is 83.2 ± 1.2 km with a slight tendency toward lower altitudes for brighter clouds (Fiedler et al., 2009). The mean altitude of the maximum ice mass density from SOFIE observations in 2007 lies at 82.9 km (Hervig et al., 2009b). Given the different sensitivities of the instruments and the different spatial and temporal coverages, these mean altitudes agree fairly well.

Based on SOFIE observations presented by Hervig et al. (2009b), where all profiles were aligned so that the altitude of maximum extinction z_{max} falls on the July average, the number of ice particles is fairly constant above z_{max} with 200 to 300 cm^{-3}. It is only below z_{max}, that is, below the maximum ice mass density, that the number of ice particles decreases significantly. This region coincides with a further growth of the ice particle radii. If there is something as a "growth region," where few particles grow on the expense of others, this growth region would be below z_{max}. However, this part of the cloud has a significantly lower ice mass density and is unlikely to produce bright NLCs, since we expect β_{max} to be close to the maximum ice mass density.

This means that the observable part of the cloud, namely, the region of maximum ice mass density and presumably also β_{max} lies above a "growth region." In such a case, the ice number density in the brightest part of the cloud would be coupled to the ice number density at nucleation heights, thus favoring the vertical wind

concept. However, a more detailed analysis with further data sets is required before any definite conclusions can be drawn about the dominating concept.

4. Conclusion

Even though M19 concludes that the results of M11 and WRK16 are rather similar, we do not agree on that. We find a clear linear relationship connecting the number densities of CN with (1) the ice particle number densities at the altitude of maximum cloud brightness and (2) with the ice column mass. Our results thus demonstrate a strong sensitivity of the observable cloud properties on the nucleation conditions.

These seemingly opposing results from M11 and WRK16 can be unified by taking the vertical wind amplitude into account. We speculate that the relative contribution of wind and diffusion to the vertical transport decides whether NLC properties are sensitive to the nucleation conditions or not. Since vertical wind amplitudes are not well constrained in the mesopause region and may vary locally and temporally, no final conclusion can be drawn on which concept is more realistic. For that, detailed statistics of vertical wind amplitudes would be required in combination with further analyses of satellite and lidar observations. Modeling studies dedicated to this question should comprise eddy diffusion coefficients which are consistent with the gravity wave background fields.

References

Becker, E. (2009). Sensitivity of the upper mesosphere to the Lorenz energy cycle of the troposphere. *Journal of the Atmospheric Sciences*, *66*, 647–666. https://doi.org/10.1175/2008JAS2735.1

Fiedler, J., Baumgarten, G., & Lübken, F.-J. (2009). NLC observations during one solar cycle above ALOMAR. *Journal of Atmospheric and Solar-Terrestrial Physics*, *71*(3-4), 424–433. https://doi.org/10.1016/j.jastp.2008.11.010

Hervig, M. E., Gordley, L. L., Deaver, L. E., Siskind, D. E., Stevens, M. H., Russell, J. M., et al. (2009a). First satellite observations of meteoric smoke in the middle atmosphere. *Geophysical Research Letters*, *36*, L18805. https://doi.org/10.1029/2009GL039737

Hervig, M. E., Gordley, L. L., Russell, J. M. III, & Bailey, S. M. (2009b). SOFIE PMC observations during the northern summer of 2007. *Journal of Atmospheric and Solar-Terrestrial Physics*, *71*, 331–339. https://doi.org/10.1016/j.jastp.2008.08.010

Hunten, D. M., Turco, R. P., & Toon, O. B. (1980). Smoke and dust particles of meteoric origin in the mesosphere and stratosphere. *Journal of the Atmospheric Sciences*, *37*(6), 1342–1357.

Megner, L. (2011). Minimal impact of condensation nuclei characteristics on observable Mesospheric ice properties. *Journal of Atmospheric and Solar-Terrestrial Physics*, *73*, 2184–2191. https://doi.org/10.1016/j.jastp.2010.08.006

Megner, L. (2019). Comment on "Nucleation of mesospheric cloud particles: Sensitivities and limits". *Journal of Geophysical Research: Space Physics*, *124*. https://doi.org/10.1029/2018JA025646

Megner, L., Siskind, D. E., Rapp, M., & Gumbel, J. (2008). Global and temporal distribution of meteoric smoke: A two-dimensional simulation study. *113*, D03202. https://doi.org/10.1029/2007JD009054

Pruppacher, H. R., & Klett, J. D. (1997). *Microphysics of clouds and precipitation* (2nd ed.). Dordrecht and Boston: Kluwer Academic Publishers.

Rapp, M., & Thomas, G. E. (2006). Modeling the microphysics of mesospheric ice particles: Assessment of current capabilities and basic sensitivities. *Journal of Atmospheric and Solar-Terrestrial Physics*, *68*(7), 715–744. https://doi.org/10.1016/j.jastp.2005.10.015

Wilms, H., Rapp, M., & Kirsch, A. (2016). Nucleation of mesospheric ice particles: Sensitivities and limits. *Journal of Geophysical Research: Space Physics*, *121*, 2621–2644. https://doi.org/10.1002/2015JA021764

References from the Supporting Information

Becker, E., & Vadas, S. L. (2018). Secondary gravity waves in the winter mesosphere: Results from a high-resolution global circulation model. *Journal of Geophysical Research: Atmospheres*, *123*, 2605–2627. https://doi.org/10.1002/2017JD027460

Hoffmann, P., Becker, E., Singer, W., & Placke, M. (2010). Seasonal variation of mesospheric waves at northern middle and high latitudes. *Journal of Atmospheric and Solar-Terrestrial Physics*, *72*(14-15), 1068–1079. https://doi.org/10.1016/j.jastp.2010.07.002